

pubs.acs.org/jnp Note

Advanced Structure Analysis Reveals a Transient Portimine B Hydrate

Jared S. Wood, Junchen Tang, Wendy K. Strangman,* and R. Thomas Williamson*



Cite This: https://doi.org/10.1021/acs.jnatprod.4c00525



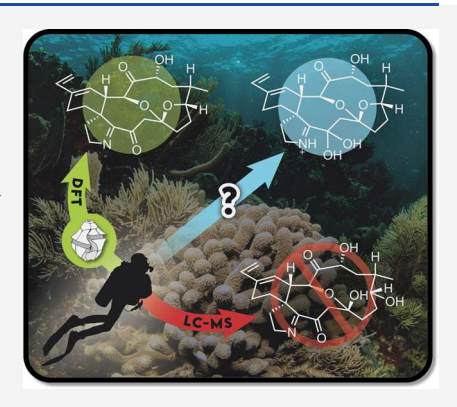
ACCESS I

III Metrics & More

Article Recommendations

SI Supporting Information

ABSTRACT: Portimine B was isolated from an extract derived from the dinoflagellate *Vulcanodinium rugosum*, a known producer of the closely related portimine A. Initial molecular characterization studies of portimine B suggested an open tetrahydrofuranyl ring isomer, contrary to the intact ring moiety found in portimine A. In 2023, the Baran lab synthesized both portimines A and B suggesting that both macrocyclic analogs contained the intact tetrahydrofuranyl ring. In this note, we utilize newly acquired NMR data, the i-HMBC NMR experiment, and advanced density functional theory calculations to define the structural divergence, originating from the presence of a transient hydrate.



Since the isolation and characterization of portimine A (Figure 1, 1) from the dinoflagellate *Vulcanodinium* rugosum (V. rugosum) in 2013, the molecule has attracted considerable attention, first due to its association with harmful algal blooms, and later due to noteworthy anticancer activity. The cyclic imine moiety of the macrocyclic structure of portimine A (1) is a defining characteristic of a steadily growing group of marine toxins defined by this unusual

Portimine A (1)

Calculated Mass: [M+H]* 402.2275

Natural Reported: [M+H]* 418.2230

Natural Reported: [M+H]* 418.2230

Natural Reported: [M+H]* 418.2230

Natural Reported: [M+H]* 418.2230

Synthetic Reported: [M+H]* 400.2117

Figure 1. Structures 1-3 highlight confounding spectroscopic, spectrometric, and chromatographic data from the original structure elucidation report. Arrow denotes a key ${}^3J_{\rm CH}$ correlation observed for portimine A (1) that was below the limit of detection in the original portimine B (3) data that ultimately established the closed ring tetrahydrofuranyl core.

structural motif.³ In addition to portimines, notable examples include the gymnodimines, spirolides, pinnatoxins and pteriatoxins, which all contain the characteristic imine functional group and spiro-linked rings.³ These unusual compounds are produced primarily by several marine dinoflagellate genera and have been detected in shellfish and seafood worldwide.

In 2019, portimine B (Figure 1, original structure 2), a closely related oxidized analog of portimine A (1), was reported along with a detailed study of its cell permeable apoptotic activity against oral carcinoma. In 2023, the Baran group published a notable synthesis of both portimine A (1) and portimine B (Figure 1, revised structure 3). In that work, the structure of portimine A (1) was confirmed as reported but the structure of portimine B (3) was revised to the closed ring tetrahydrofuranyl tautomer. This seminal work provided material for further study and allowed determination of the mechanism of action for these compounds utilizing a state-ofthe-art proteomics approach.5 While the synthesis left vanishingly small doubt regarding the true identity of portimine B (3), there remained several unresolved inconsistencies related to the original molecular characterization studies. In this report, we dissect these incongruities and apply advanced structure elucidation tools and the latest advances in

Received: May 6, 2024 Revised: July 16, 2024 Accepted: July 17, 2024



density functional theory (DFT) calculations to provide orthogonal conformation of its identity and offer convincing evidence that reconciles the apparent structural divergence between the natural product and the synthetic material. In doing so, we also demonstrate how these tools can be used in conjunction with more routine methods to ensure the highest level of confidence in the structural characterization of known and newly isolated natural products.

The first piece of incongruous data in the structural identification of portimine B (3) was the QToF-HRMS spectrum (m/z 418.2230⁺) which provided the original working molecular formula ($C_{23}H_{32}NO_6$) from what was believed to be the [M + H]⁺ molecular ion (Figure 1). This molecular formula has the same nine degrees of unsaturation recognized in portimine A (1) but, accounting for the ketone identified in the 1D ¹³C for portimine B (3), necessitated one less ring as proposed in structure (2).

Another unusual observation in the isolation of portimine B (3) was its behavior on typical reversed phase chromatography media (Figure 2). The structures of portimine A (1) and

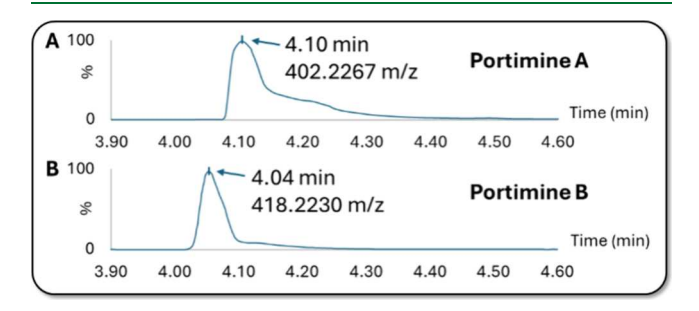
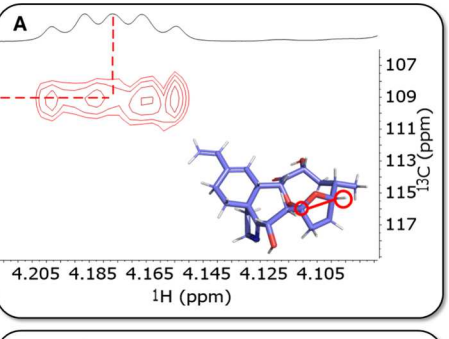


Figure 2. RP-HPLC traces of (A) portimine A (1) and (B) natural portimine B (3) in acidified mobile phase.

revised structure of portimine B (3) are identical except for the oxidation state at C-5; a hydroxy group in (1), and a carbonyl in (3). Based on this structural information, the generally accepted order of elution is that portimine A (1) would be more polar and would therefore elute first. Yet, it was observed that (3) eluted ahead of (1) on standard C18 stationary phase with a solvent system composed of aqueous acetonitrile.

Both the initially proposed and corrected structures displayed remarkably similar NMR chemical shift predictions that only later could be clearly disentangled using advanced DFT methods. Additionally, a key observation that appeared to support structure (2) was the absence of an HMBC correlation across the tetrahydrofuranyl oxygen ring from H-10/C-7 (Figure 1). This through-heteroatom $^3J_{CH}$ correlation was readily observed in the portimine A (1) control experiment but no sign of a response was noted in the original work, even with the application of various data processing schemes aimed at increasing the overall S/N for this key correlation (Figure 3).

Based on the anomalous results detailed above, we initiated a study to investigate these data with a fresh mind to evaluate whether newer instrumentation and methodologies would have helped to avoid the mischaracterization of portimine B (3). The first step in this study was to acquire 1H NMR data for a 25 μ g voucher sample of natural portimine B (3) and compare that with the synthetic material prepared by the Baran lab. These two samples were also combined and shown to be identical (see Supporting Information Sections S3 and S4). Next, we revisited the LC-QToF-MS spectrum for the natural and combined natural/synthetic samples. Not surprisingly, the



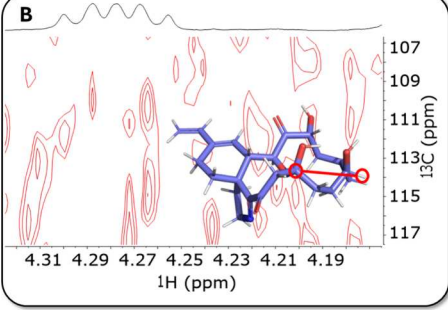


Figure 3. (A) HMBC correlation from H-10/C-7 for portimine A (1). (B) Absence of observable HMBC correlation from H-10/C-7 at maximum magnification for portimine B (3), thus suggesting the originally proposed structure (2).

natural and combined samples both exhibited the same previously observed ion at 418.2230 $^{+}$ (30% CH $_3$ CN:0.1% formic acid (FA)/70% H $_2$ O:0.1% FA), in full agreement with the original report. When this molecular ion was selected for further MS-MS fragmentation, the next most abundant fragment ion was observed at 400.2110 suggesting loss of water from the precursor peak as the molecule reverted back to the native portimine B (3) structure. Following these tests, we next turned our attention to reacquisition of the most critical NMR data.

HMBC data were acquired on 1.2 mg of portimine B (3) using a 5 mm nitrogen cooled cryoprobe. With the increased S/N compared to the data originally acquired, surprisingly, a weak but clear correlation was noted for the $^3J_{\rm CH}$ H-10/C-7 heteronuclear coupling. Acquisition of an HMBC data set on portimine A (1) with identical experimental parameters revealed a very similar response for the same primary scalar coupling of interest. For a more accurate comparison, the ratios of the through-oxygen correlation from H-15/C-7 were compared to H-10/C-7 for both analytes. Interestingly, these intensities were quite comparable at 100:10 for portimine A and 100:5 for portimine B (3) (Figure 4).

The fact that no H-10/C-7 correlation was observed in the original data can be attributed to a combination of the inherently weak response for that ${}^3J_{\rm CH}$ in the HMBC data coupled with marginal signal-to-noise in the overall data set. This peculiar discrepancy may specifically result from an antiphase cancellation of the expected coupling during the HMBC experiment (see Supporting Information Section S10).

The unexpected comparability of the relative magnitude for H-10/C-7 responses prompted us to take a closer look at the NMR chemical shift data for portimine A (1) and B (3). Toward this end, we initiated detailed DELTAS0⁶ based DFT NMR chemical shift calculations for the consensus structure for portimine A (1), the original proposed structure for

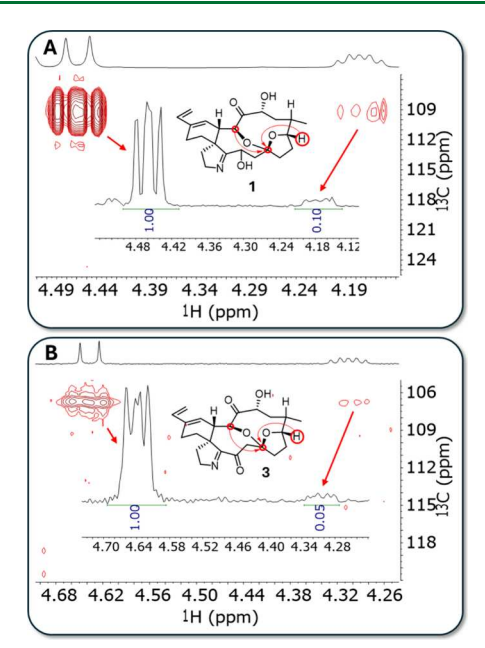


Figure 4. Comparison of HMBC data for (A) portimine A (1) and (B) portimine B (3) synthetic material highlighting the horizontal slices taken through the C-7 ¹³C resonance.

portimine B (2), and the revised structure for portimine B (3). These results clearly pointed toward strong agreement with the portimine A (1) structure (RMSD for $^{1}H = 0.18$ ppm and for $^{13}C = 3.4$ ppm) and the closed tetrahydrofuranyl ring present in the revised structure for portimine B (3) (RMSD for $^{1}H = 0.08$ ppm and for $^{13}C = 2.1$ ppm) while suggesting significant incongruities in proximity of the open ring structure (2) from the original report (RMSD for $^{1}H = 0.26$ ppm and for $^{13}C = 5.0$ ppm) (Figure 5). Total nuclear spin—spin coupling constants (*J*) were calculated at the mPW1PW91/6-311++G(2d,p) level of theory using geometry-optimized structures of portimines A (1) and B (3), and it was interesting to note that the coupling constant predictions from H-10/C-7 were virtually identical for both compounds (~4.5 Hz).

With these new data in hand, it became apparent that the origin of the divergence between the original proposed structure and revised structure was manifest between the liquid chromatography used for mass spectrometric analysis and isolation and subsequent NMR analysis. Therefore, we hypothesized that the acidic aqueous media used in the chromatography may have led to the reversible formation of a hydrate at the site of the former C-5 ketone (Figure 6, 4). It was deemed that the reactivity of this ketone would be enhanced by the neighboring imine carbon, analogous to α -keto acids that are known to exhibit equilibrium between the gem-diol and the parent ketone and in an equilibrium that generally shifts to around 2:1 in the former when dissolved in acidic media.

To probe the validity of this hypothesis, a 1H NMR spectrum was acquired in CD₃CN before and after the addition of H₂O with 0.1% FA. Upon addition of the acidic media, we observed significant shifts in the 1H NMR data, especially for the doublet 1H NMR resonances for H₂-6 (Figure 6). An HMBC spectrum was acquired, and as expected, it revealed a dramatic ~ 100 ppm change in chemical shift for C-5 (201.4 ppm for 3 to 92.5 ppm for 4) providing strong evidence for the formation of the proposed hydrate

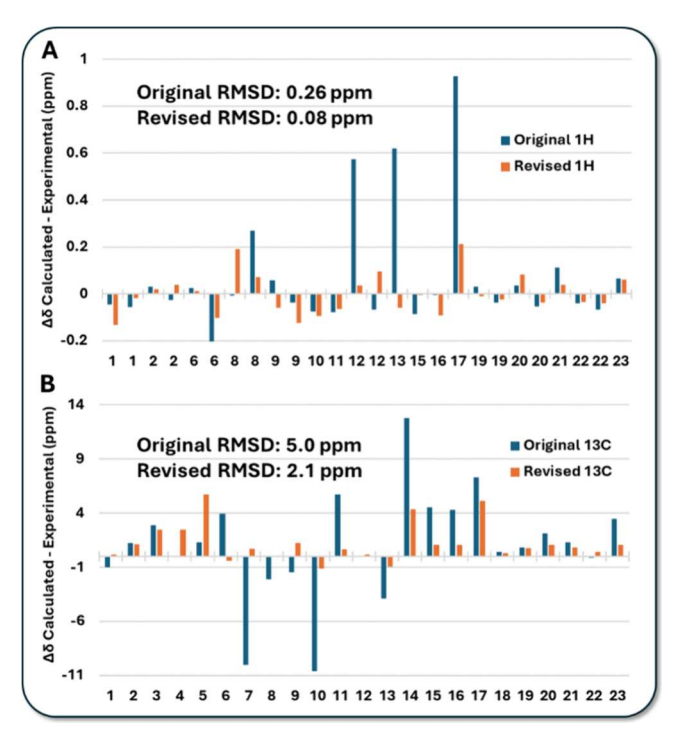


Figure 5. $\Delta\delta$ bar graphs for DFT analysis of portimine B, including atom numbers. (A) 1 H chemical shift error bars for the original (2) and revised (3) structures of portimine B. (B) 13 C chemical shift error bars for the original (2) and revised (3) structures of portimine B.

intermediate. As postulated, the hydrate reverted to the ketone upon drying under a stream of liquid nitrogen (see Supporting Information Section S14).

One additional transient structure possibility that could not yet be eliminated was the alternate generation of a hemiaminal/ketone structure (Figure 6, 5) rather than the imine/ gem-diol structure (4). These possibilities were evaluated through i-HMBC analysis, which was used to distinguish ²J_{CH} vs ³J_{CH} correlations by comparing the proton chemical shifts from the 1D proton NMR, in which ~98.9% of protons are adjacent to exclusively 12C nuclei, versus the proton chemical shifts observed in the HMBC experiment, in which the protons are either 2- or 3-bonds away from an isolated ¹³C nucleus. The magnitude of this chemical shift difference (the so-called "isotope shift") is a function of the distance from the ¹³C nucleus. In practice, this evaluation is typically carried out by direct comparison of the difference between two- and threebond isotope shifts $(^{2-3}\Delta^1H(^{13/12}C))$. To execute this analysis, the 4K \times 128 pts HMBC data were linear predicted to 8K \times 128 pts and zero filled to $16K \times 512$ pts. Slices of HMBC data for correlations from H-6 to C-4, C-7, and C-5 are shown below (Figure 7). Peaks were identified via line fitting to establish an absolute center point (isotope shift) for each multiplet, and their differences correspond to $^{2-3}\Delta^{1}H(^{13/12}C)$. In general, it is expected that isotope shift differences for ${}^2J_{CH}$ are larger than that of ${}^{3}J_{CH}$, and that they are typically (but not always) greater in magnitude than 0.30 ppb. All isotope shift differences must be measured relative to the most downfield multiplet center in the HMBC data. In this case, the measured $^{2}J_{CH}$ isotope shift difference for H-6 to the acetal carbon C-7 served as a convenient reference for comparison to the potential ${}^{2}J_{CH}$ isotope shift difference for H-6 to C-4 or C-5. As can be seen in Figure 7, the latter HMBC correlation (H-6/C-

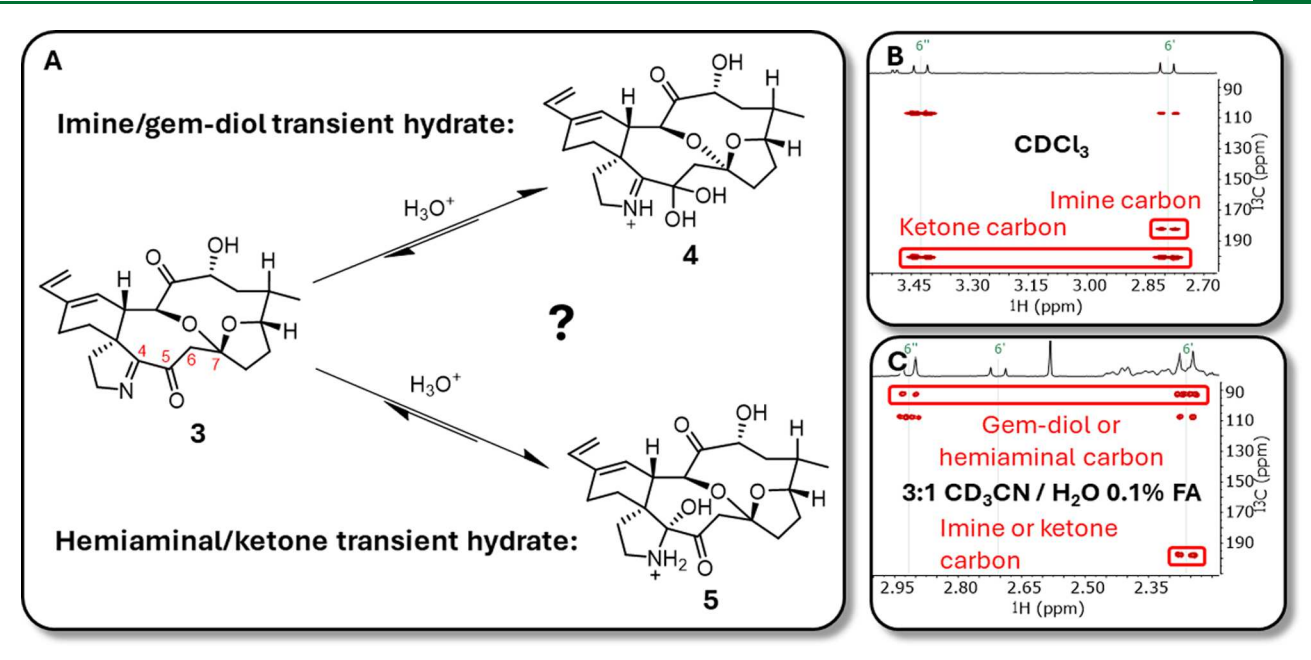


Figure 6. HMBC data comparing resonance shifts in the presence of acidic media. (A) Schematic showing the potential formation of the gem-diol structure (4) or hemiaminal structure (5). (B) HMBC data for portimine B (3) collected in CDCl₃. (C) HMBC data collected in 3:1 CD₃CN/ $_{10}$ O with 0.1% FA.

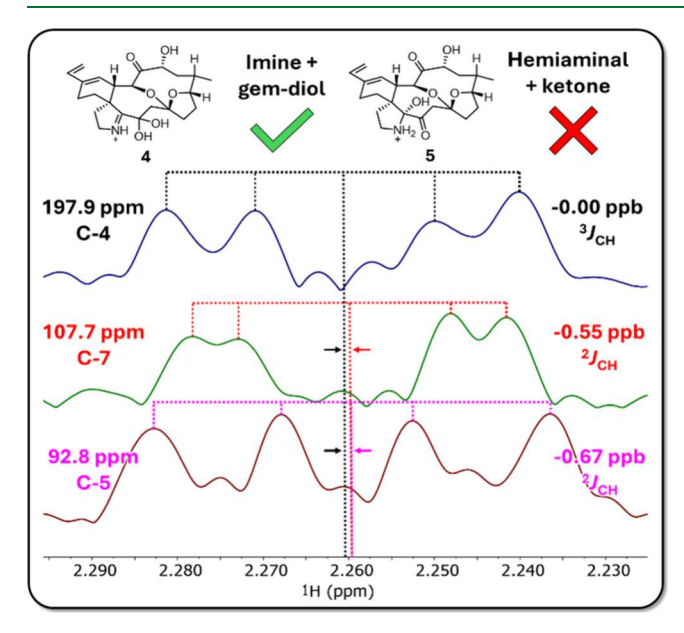


Figure 7. i-HMBC analysis of the transient hydrate structure of portimine B (4), highlighting correlations from H-6 to C-4, C-7, and C-5, noting isotope shift differences to distinguish $^2J_{\rm CH}$ vs $^3J_{\rm CH}$ correlations.

5) exhibited a relative two-bond isotope shift difference of -0.67 ppb (compared to the ${}^{3}J_{\rm CH}$ H-6/C-4 response) that clearly coincided with the two-bond connectivity, thus confirming the imine/gem-diol structure (4).

To further support the proposed hydrate, chemical shift calculations for the neutral and protonated variants of the imine/gem-diol (4) and hemiaminal/ketone (5) structures were carried out based on methods reported by Pierens for acetonitrile. Atoms C-4, C-7, and C-5 were evaluated for both structure candidates. Interestingly, the neutral species exhibited calculated chemical shifts of 188.2, 110.7, and 95.4 ppm for C-4, C-7, and C-5, respectively, whereas the protonated species

yielded 213.4, 108.5, and 97.3 ppm for those same carbons. The calculated pK_a (ACD Laboratories Inc.) for portimine B (3) in the presence of formic acid suggested that roughly 50% of the analyte would be protonated under these conditions. An average of the predicted chemical shifts for the neutral/protonated species compared to the experimental chemical shifts leads to absolute errors of 3.0 ppm for C-4, 2.0 ppm for C-7, and 3.8 ppm for C-5, all well within expected accuracy for DFT calculations of chemical shifts that were experimentally recorded in a mixed aqueous/organic solvent. For the hemiaminal/ketone structure (5), absolute errors were 8.0 ppm for C-4, 1.9 ppm for C-7, and 11.3 ppm for C-5 (see Supporting Information S21). Overall, these data fully support the imine/gem-diol structure (4).

Herein we have investigated the origin of structural ambiguity between synthetically prepared portimine B (3) and the spectroscopically characterized natural product. The confusion and apparent inconsistencies in molecular characterization data can be attributed to the in situ formation of a hydrate during chromatography steps preceding mass spectrometric analysis and preparative isolation of material for NMR, PAMPA permeability, and biological assays.5 Thus, it should be noted that portimine B (3) will show up in LC-MS spectra as the intermediate with a characteristic [M+18]⁺ ion under acidic conditions that are commonly recommended for this work. At least one other similar example can be found in the literature for the structural revision of a synthetic product, homolongamide. 10 In that case, the decoy product was found to be a methanol solvation product which formed a hemiacetal. With today's nearly ubiquitous application of high and low pH mobile phase modifiers, the natural products community would be well-served to exercise caution when working in the presence of aldehydes, ketones, or other labile functional groups.

■ EXPERIMENTAL SECTION

General Experimental Procedures. The original NMR data were collected using a Bruker Avance 1 500 MHz system equipped with a 1.7 mm TXI room temperature probe using TopSpin version 2.0. The NMR data recorded in the present study were acquired using a Bruker Neo NMR spectrometer operating at a ¹H observation frequency of 499.861999 MHz and equipped with a H/F C/N TCI 5 mm Prodigy CryoProbe using TopSpin version 4.1.4. The HRMS spectrum was obtained on Waters UPLC I-Class system coupled to a Waters Xevo-G2XS QToF-MS mass spectrometer. LC-MS monitoring of chromatography fractions was performed on a Waters QDa mass detector tandem to a Waters I-Class UPLC PDA instrument. HPLC isolation was performed using a Waters Breeze HPLC system with a Waters dual wavelength detector (210 and 240 nm).

NMR Spectroscopy. In the original report, samples were prepared and analyzed in 1.7 mm NMR tubes with 50 μ L solvent and all spectra were acquired at room temperature in CDCl₃ (Cambridge Isotope Laboratories).⁴ Data acquired for this work were prepared in 3 mm NMR tubes with 150 μ L solvent. All data were acquired at 25 °C in CDCl₃ (Cambridge Isotope Laboratories) excluding the hydrate formation data, which was acquired in 3:1 CD₃CN (Cambridge Isotope Laboratories)/H₂O with 0.1% formic acid (Honeywell). ¹H NMR data was referenced to 7.26 and 1.94 ppm for CDCl₃ and CD₃CN, respectively. HMBC experiments were optimized for $^{n}J_{CH}$ = 8 Hz and were acquired with 4096 points in the direct dimension (16K points in postprocessing) and 128 points in the indirect dimension (512 points in postprocessing). Nonuniform sampling (NUS) with strictly random sampling was used for the acquisition of HMBC data; 50% of data points were collected for these experiments. All NMR data were processed in MestReNova (version 15.0.0). For i-HMBC analysis, peaks were picked with the line-fitting tool, using a width constraint of 0.10 to 100.00 Hz, a position constraint of ± 1.00 Hz, a generalized Lorentzian shape, a maximum of 5000 coarse prefitting iterations, a maximum of 5000 fine iterations, and a local minima filter value of 5.

Mass Spectrometry. The UPLC-MS system was operated in electrospray positive mode (ESI $^+$) with the capillary voltage set at 2.5 kV, source and desolvation temperatures at 100 and 550 $^{\circ}$ C respectively and desolvation gas flow at 800 L/h. MS-MS data were acquired with the same instrument under the same conditions with a set mass of 418.2 and a collision energy of 35 eV. All solvents were of LC-MS grade and used without further purification.

Isolation of Portimines A and B. Portimines A (1) and B (3) were fractionated on HP20, LH20 and subsequently purified by HPLC on YMC Pack ODS-AM 5 μ m × 12 nm 250 × 10 mm column under isocratic conditions (30% MeCN:70% H₂O, 0.05% formic acid, 2.5 mL/min; RT 1, 11.4 min; RT 2, 10.8 min:). All solvents were of HPLC grade and were used without further purification.

Conformational Search and DFT Calculation of NMR Parameters. For DFT calculations, ChemDraw structures were energy-minimized in Chem3D, and the Schrödinger MacroModel software package was used to perform a mixed torsional/low-mode sampling (MTLMOD) conformational search using the OPLS4 force field. 11 Chemical shift (δ) calculations for structures 1–3 were carried out following the DELTAS0^6 methodology; specifically, ^1H δ calculations were performed at the WP04/6-311++G(2d,p)// B3LYP-D3/6-311G(d,p) level of theory, and 13 C δ calculations were performed at the ωB97X-D/def2-SVP//B3LYP-D3/6-311G-(d,p) level of theory, both including the integral equation formalism polarizable continuum model (IEFPCM) for the optimization and NMR δ prediction stages of the calculations. Boltzmann weighting was performed using geometry-optimized energies, and no imaginary frequencies were present. δ calculations for structures 4 and 5 were carried out following methods reported by Pierens⁹ for acetonitrile; specifically, 1 H δ calculations were performed at the WP04/aug-ccpVDZ//B3LYP/6-31+G(d,p) level of theory, and 13 C δ calculations were performed at the mPW1PW91/6-311+G(2d,p)/B3LYP/6-31+G(d,p) level of theory, with IEFPCM used for the 1 H NMR δ prediction stage of the calculations. As was done for structures 1-3, Boltzmann weighting was performed using geometry-optimized energies, and no imaginary frequencies were present.

ASSOCIATED CONTENT

Data Availability Statement

The NMR data for compounds 3 and 4 have been deposited in the Natural Products Magnetic Resonance Database (NP-MRD; www.np-mrd.org) and can be found at NP0333598 (portimine B, 3) and NP0333599 (portimine B hydrate, 4).

Supporting Information

The Supporting Information is available free of charge at https://pubs.acs.org/doi/10.1021/acs.jnatprod.4c00525.

Experimental details, 1D and 2D NMR spectra, HR-ESI-MS spectra, δ assignments, and DFT calculation results (PDF)

AUTHOR INFORMATION

Corresponding Authors

- R. Thomas Williamson Department of Chemistry and Biochemistry, University of North Carolina Wilmington, Wilmington, North Carolina 28409, United States; orcid.org/0000-0001-7450-3135; Email: williamsonr@uncw.edu
- Wendy K. Strangman Department of Chemistry and Biochemistry, University of North Carolina Wilmington, Wilmington, North Carolina 28409, United States;
 Occid.org/0000-0002-6911-4909; Email: strangmanw@uncw.edu

Authors

Jared S. Wood – Department of Chemistry and Biochemistry, University of North Carolina Wilmington, Wilmington, North Carolina 28409, United States; ○ orcid.org/0000-0002-3940-0461

Junchen Tang – Department of Chemistry, The Scripps Research Institute, La Jolla, California 92037, United States

Complete contact information is available at: https://pubs.acs.org/10.1021/acs.jnatprod.4c00525

Notes

The authors declare no competing financial interest.

■ ACKNOWLEDGMENTS

NSF Grant Nos. 0821552 and 2116395 are acknowledged for the NMR spectrometers utilized in this work. Helpful discussions with Ryan D. Cohen, Xiao Wang, Gary E. Martin, and Carlos Jiminez are acknowledged. Phil S. Baran is acknowledged for providing materials.

DEDICATION

This work is dedicated to D. John Faulkner, who always promoted the value of meaningful structure revisions.

REFERENCES

- (1) Selwood, A. I.; Wilkins, A. L.; Munday, R.; Shi, F.; Rhodes, L. L.; Holland, P. T. *Tetrahedron Lett.* **2013**, *54*, 4705–4707.
- (2) Cuddihy, S. L.; Drake, S.; Harwood, D. T.; Selwood, A. I.; McNabb, P. S.; Hampton, M. B. *Apoptosis.* **2016**, *21*, 1447–1452.
- (3) Stivala, C. E.; Benoit, E.; Araoz, R.; Servent, D.; Novikov, A.; Molgo, J.; Zakarian, A. *Nat. Prod. Rep.* **2015**, *32*, 411–435.
- (4) Fribley, A. M.; Xi, Y.; Makris, C.; Alves-de-Souza, C.; York, R.; Tomas, C.; Wright, J. L. C.; Strangman, W. K. ACS Med. Chem. Lett. **2019**, 10, 175–179.

- (5) Tang, J.; Li, W.; Chiu, T.-Y.; Martinez-Pena, F.; Luo, Z.; Chong, C. T.; Wei, Q.; Gazaniga, N.; West, T. J.; See, Y. Y.; Lairson, L. L.; Parker, C. G.; Baran, P. S. *Nature* **2023**, *622*, 507–513.
- (6) Cohen, R. D.; Wood, J. S.; Lam, Y.-H.; Buevich, A. V.; Sherer, E. C.; Reibarkh, M.; Williamson, R. T.; Martin, G. E. *Molecules* **2023**, 28, 2449.
- (7) Cooper, A. L.; Redfield, A. G. J. Biol. Chem. 1975, 250, 527-532.
- (8) Wang, Y.; Fan, A.; Cohen, R. D.; Dal Poggetto, G.; Huang, Z.; Yang, H.; Martin, G. E.; Sherer, E. C.; Reibarkh, M.; Wang, X. *Nat. Commun.* **2023**, *14*, 1842.
- (9) Pierens, G. K. J. Comput. Chem. 2014, 35, 1388-1394.
- (10) Barrios Sosa, A. C.; Yakushijin, K.; Horne, D. A. Tetrahedron Lett. 2000, 41, 4295–4299.
- (11) Lu, C.; Wu, C.; Ghoreishi, D.; Chen, W.; Wang, L.; Damm, W.; Ross, G. A.; Dahlgren, M. K.; Russell, E.; Von Bargen, C. D.; Abel, R.; Friesner, R. A.; Harder, E. D. *J. Chem. Theory. Comput.* **2021**, 17, 4291–4300.